

PHYSICAL REVIEW B

CONDENSED MATTER

THIRD SERIES, VOLUME 40, NUMBER 2

15 JULY 1989-I

Location of hydrogen adsorbed on palladium (111) studied by low-energy electron diffraction

T. E. Felter and Erik C. Sowa*

Sandia National Laboratories, Livermore, California 94551-0969

M. A. Van Hove

Materials and Chemical Sciences Division, Lawrence Berkeley Laboratory, Berkeley, California 94720

(Received 9 January 1989)

Low-energy-electron-diffraction (LEED) I - V curves have been measured for H adsorbed on Pd(111) in the $(\sqrt{3}\times\sqrt{3})R30^\circ\text{-}2\text{H}$ structure, which occurs at a coverage $\Theta = \frac{2}{3}$. The measurements are compared to calculations using dynamical LEED techniques. Twenty-one distinct geometry types were investigated, each one with metal-interlayer relaxations allowed and the distance of the H atom above (or below) the top Pd layer varied. The metal-interlayer spacings that we find are within error bars of those of the clean surface. Agreement between theory and experiment was achieved for structures with one of the two H atoms in the unit mesh in a threefold hollow surface site, above third-layer metal atoms (denoted "A +"). The second H resides either in the same type of site or in another type of threefold site, such as the hollow surface site above second-layer metal atoms B + or the subsurface sites between first- and second-layer metal atoms, A - or B -. We find that good reliability factors R are achieved for subsurface occupation fractions up to 60%. The results are consistent with the embedded-atom-method prediction of substantial subsurface H and with previous electron-stimulated desorption measurements.

INTRODUCTION

The interaction of hydrogen with metal surfaces continues to attract a considerable amount of theoretical and experimental attention, as recent reviews of the field attest.^{1,2} Palladium is particularly interesting because of its ready ability to form bulk phases with H, namely the solid solution or α phase and the hydride or β phase. These phases have been observed and characterized by many techniques including, recently, surface science studies in ultrahigh vacuum (UHV). Crucial to the understanding of the mechanism of hydride formation is the transition from adsorption at a surface site to a bulk site in an underlying layer.

Eberhardt *et al.* postulated penetration of H below Pd(111) (Ref. 3) as an explanation of the loss of H-induced features in the ultraviolet-photoemission spectroscopy (UPS) spectrum upon heating the specimen to temperatures less than the onset of desorption. A decrease in electron-stimulated desorption (ESD) yield under these circumstances has also recently been observed by Kubiak and Stulen and interpreted as either desorption or diffusion into regions many layers below the surface.⁴ Daw and Foiles⁵ have used the embedded-atom method (EAM)⁶ to predict the structure of H/Pd(111);

the calculated structures agree with the symmetry of the low-energy-electron-diffraction (LEED) patterns and with the corresponding disordering temperatures.⁷ Their calculations indicate that subsurface sites (i.e., sites between the first and second layers of the substrate), as well as surface sites, are populated even during low-temperature adsorption. At low temperature (75 K) and a coverage of $\Theta = 2/3$, approximately 33% of the adsorbed H is predicted by the EAM to be on the surface in threefold hollow sites above third-layer metal atoms and 67% to be subsurface in octahedral sites between the first and second metal layers (in the present work these sites are denoted A + and A -, respectively). As the temperature is raised, the distribution approaches complete randomization (50% surface and 50% subsurface), so more H is on the surface and a higher ESD yield is expected. Kubiak and Stulen⁴ found such an increase in the ESD yield between 75 and 150 K.

The present work was strongly motivated by the predictions of the EAM and explores by dynamical LEED intensity analysis the possibility of subsurface H on Pd(111) for the structure at $\Theta = \frac{2}{3}$, which is identified by the notation $(\sqrt{3}\times\sqrt{3})R30^\circ\text{-}2\text{H}$. This structure is the second of two superstructural arrays found for H on Pd(111). Both arrays have $(\sqrt{3}\times\sqrt{3})R30^\circ$ symmetry,

but the first contains one H atom in the unit mesh with a coverage $\Theta = \frac{1}{3}$ while the second contains two at $\Theta = \frac{2}{3}$. Both structures disorder at relatively low temperatures, 85 and 105 K, respectively.⁷ However, because cooling is more easily performed with liquid nitrogen (77 K) than with liquid helium (4 K) and because sample holders inevitably contain a few degrees of cooling losses, the second structure is considerably easier to observe than the first and was therefore chosen for this initial work.

PREVIOUS DETERMINATIONS OF RELATED STRUCTURES

Vibrational spectroscopy (mainly high-resolution electron-energy-loss spectroscopy) has been applied to many H adsorption systems. For threefold symmetric substrates, the technique has been applied to H on Ni(111),⁸ Ru(0001),^{9,10} Rh(111),¹¹ Pd(111),¹² and Pt(111).¹³ Generally, threefold hollow-site adsorption was inferred by postulating a reasonable force-constant model and comparing the number and symmetry of the vibrational modes to experiment. Usually, the technique does not permit a determination of bond length although in one case, Pt(111), a H—metal bond length of 1.76 Å was suggested.¹³ It should be realized that, because of its small mass, hydrogen is relatively delocalized on these surfaces, i.e., the zero-point motions are on the order of 1 Å parallel to the surface.^{11,14,15} As in the case of thermal motion, we focus our discussion on the average nuclear positions.

Because of the postulates and assumptions involved in vibrational studies, it is important to try to determine the adsorption structure by other means and to determine specifically the H—metal bond length. This has been done for Pt(111) (Ref. 16) by helium-atom diffraction, for Ru(0001) (Ref. 17) by very-low-energy electron diffraction (VLEED), for Ni(111) by LEED (Ref. 14), and for Ni(111) and Pd(100) by transmission-ion channeling.^{18,19} In the He-diffraction work, a Pt—H bond length of 1.9 Å was deduced with threefold hollow adsorption. In the VLEED work, H was found to sit in the threefold hollow site with the Ru—H bond length 1.91 Å at saturation and decreasing by 0.1–0.2 Å at lower coverage. For Ru(0001)/H only (1×1) and disordered structures have been analyzed to date, although a (2×2) or (2×1) structure was observed below 60 K. In the channeling study of Pd(100), it was deduced that the hydrogen was in the fourfold hollow site, with a Pd—H bond length of 2.00 and 1.97 Å for the *c*(2×2) and 1×1 structures, respectively. For Ni(111), it has recently been deduced with the same technique that for the (2×2)-2H ordered structure, both types of threefold hollow sites are equally populated. This generally confirms the original LEED work on Ni(111) which was the first structural determination of H adsorbed on a surface. The nickel—H bond was found to be 1.84±0.06 Å using LEED and 1.65±0.05 Å using transmission-ion scattering.

Other LEED structural determinations have been performed with H on Co(10 $\bar{1}$ 0) (Ref. 20) on W(100) (Ref. 21) and on the (110) surface of Fe,²² Rh,²³ Pd,²⁴ and Ni.²⁵

In these cases, as well as in the present work and the Ni(111)/H (Ref. 14) study, the structures analyzed were for coverages and conditions where substrate reconstruction did not occur. That is, the fractional order beams were very weak (only of the order of $\frac{1}{100}$ the average intensity of the integral order beams). When substrate reconstruction does occur, the fractional beams are much brighter and the information contained by their intensity-voltage (*I-V*) spectra are dominated by the scattering from the substrate, making it difficult to locate the weakly scattering H atoms by LEED.

EXPERIMENTAL DETAILS

The UHV chamber and video LEED system have been used in previous, low-temperature work (20 K) concerning H/Pd(111) (Ref. 26) but have not been described. Briefly, the stainless-steel chamber contains three layers of μ -metal magnetic shielding internal to the vacuum envelope and routinely achieves a base pressure in the low 10^{-11} Torr range with an ion pump. Final sample cleaning was accomplished by argon-ion bombardment at 1 keV with the sample at 900 K. The argon was kept pure by intermittent flashing of a titanium sublimator, and a small turbo pump was used to remove it from the chamber before turning on the ion pump. Cleanliness was verified by Auger-electron spectroscopy. The sample temperature was measured by a Chromel-Alumel thermocouple spot-welded to the edge of the sample and was constant at 82±1 K. The chamber pressure was less than 2×10^{-10} Torr during *I-V* measurement. Molecular hydrogen was dosed by backfilling the chamber at $(1-2) \times 10^{-9}$ Torr until the maximum intensity for the $(\sqrt{3} \times \sqrt{3})R30^\circ$ structure was reached.

The video camera is a silicon intensified target type (RCA Model TC 1030/H-SIT) and is operated without automatic gain. A Digital Equipment Corporation LS/11 computer, in conjunction with a computer-automated measurement and control (CAMAC) crate, ramps the voltage of the electron gun and records incident-electron-beam current (0.4 μ A or less for fractional beams, 0.1 μ A or less for integral beams) and spot intensity. The spot intensity is obtained from an Imaging Technologies Inc. Model IP 512 board set inserted in the LS/11 host computer. Usually, six different spots are tracked and their intensities measured during a single voltage ramp. The ramp is composed of 1-eV steps 2.3 sec in length during which 32 video frames are acquired.

Normal incidence of the LEED beam was used. Intensities were measured in the form of *I-V* curves for the (1,0) beam from approximately 50–300 eV, (0,1) from 50–300 eV, (1,1) from 170–300 eV, (2,0) from 200–300 eV, (0,2) from 185–300 eV, $(\frac{1}{3}, \frac{1}{3})$ from 25–200 eV, $(\frac{2}{3}, \frac{2}{3})$ from 70–220 eV, and $(\frac{1}{3}, \frac{4}{3})$ from 130–205 eV, together with most of their symmetrically equivalent counterparts. Symmetrically equivalent *I-V* curves were averaged together. The total-energy ranges for inequivalent integral and fractional spots were 845 and 400 eV, respectively.

THEORY

The multiple-scattering methods used to calculate the LEED intensities are well established and have been described fully.^{27,28} The atomic scattering potentials were represented by phase shifts. Ten Pd phase shifts used previously²⁹ were employed together with ten H phase shifts.³⁰ The real part of the inner potential (V_0) was assumed to be 10 eV, and was allowed to vary in 2-V steps by a rigid shift of the energy scale for the comparison of theory and experiment. A homogeneous imaginary part of the muffin-tin constant of -5 eV was used. The bulk Debye temperature used was 270 K, with an enhancement factor of 1.4 for the surface mean-square vibrational amplitudes. In the case of two H atoms in the same plane, the layer-diffraction matrices were generated using reverse-scattering perturbation, since scattering from H is weak. In the absence of Pd reconstruction (which was not considered), all of the other layers are Bravais-lattice layers. The layers were stacked by renormalized forward scattering.

Agreement between theoretical and experimental I - V spectra is quantified by five reliability (R) factors and their average, which include the reduced Zanazzi-Jona R factor (R_{RZJ}), the Pendry R factor (R_{PE}), and three others R_{OS} , R_1 , and R_2 .³¹ This set of five has been applied in many previous LEED studies. R factors for integral and fractional beams were investigated together and separately. In the latter case, agreement in V_0 and in optimum geometry is required and demanded for a legitimate structural solution. The various geometries considered are described in the following sections.

CLEAN Pd(111)

Since clean Pd(111) does not reconstruct, it is only necessary to consider relaxations, i.e., changes in the spacing between layers. As in a previous clean Pd(111) study,²⁹ we varied the top two interlayer spacings as well as the bulk interlayer spacing independently. Interlayer spacings are expressed as deviations from the standard bulk value of 2.246 Å, which assumes a cubic lattice constant of 3.89 Å. The first two parameters (Δd_{12} and Δd_{23}) were varied from the bulk value by -0.10 to $+0.10$ Å in 0.025-Å steps, and the third (Δd_{bulk}) over the same range in 0.05-Å steps. A minimum R factor of 0.166 was found for $\Delta d_{12} = +0.025$ Å, $\Delta d_{23} = 0.00$ Å, and $\Delta d_{34} = 0.00$ Å, with errors of ± 0.05 Å. Because this was a pronounced R -factor minimum, and the corresponding geometry agrees within error bars with the clean, room-temperature Pd(111) surface geometry obtained previously by LEED,²⁹ no further structural variations for the clean surface were examined. As has been noted before, the expansion of the last Pd layer is unusual;²⁹ most clean metal surface have the outermost layer spacing bulklike or contracted. However, the magnitude of the expansion is small: $+0.025$ Å corresponds to an expansion of only 1.1% and is within the error bars of an ideal truncation of the bulk.

The apparent, and unusual, expansion of the last metal layer for the clean Pd(111) surface both in the room-temperature study,²⁹ as well as the present work at low temperature, deserves some discussion. Expansion of the

palladium lattice is well known for bulk PdH_{*x*}. When hydrogen is absorbed into bulk palladium to saturate the α -phase PdH_{0.03}, the interlayer spacing increases from 2.2465 to 2.2482 Å near room temperature corresponding to an expansion of 0.08%.³² Continued absorption, in the range $x=0.03$ to approximately 0.60, takes place in the two phase region of coexistence of α (solid-solution) and β (hydride) phases. The interlayer spacing for the β phase in this region is 2.3244 Å or an expansion 3.5% relative to the pure metal. Further expansion occurs in the pure β phase for stoichiometries larger than 60% hydrogen. Thermal expansion is small, only about 0.2% from 100 to 300 K. Predictions of the embedded-atom method also indicate hydrogen-induced expansion (relative to the clean termination).⁵ In the EAM formalism, the outermost metal layer embeds itself into a higher electron density by moving toward the second layer, thereby lowering the energy. For Pd(111), the EAM calculates a contraction of the top layer spacing by 0.07 Å, 3%; as H is added to the surface, the calculated contraction is reduced, so that at $\Theta = \frac{1}{3}$, the outermost layers of Pd are separated by approximately the bulk value.⁵

In view of the expansion of the bulk upon the introduction of hydrogen and the predicted expansion at the surface⁵ with hydrogen, one possible explanation to consider for the experimental observation of a slightly expanded layer on the "clean" surface is that H is inadvertently present.²⁹ However, if H is indeed present on our clean, cold sample, it is not present in sufficient quantity to form ordered arrays since fractional beams are observed only after intentional dosing from the gas phase. The annealing temperatures and times that have been used are well above conditions for rapid decomposition of the solid-solution and hydride phases and for the desorption of the chemisorbed state.³³ It is unlikely that there could be a state of hydrogen near the surface that would survive these annealing procedures. The cool-down times of approximately two minutes or less do not permit adsorption of much residual hydrogen at the system pressure immediately following cleaning anneals, 2×10^{-10} Torr. In any case, it is important to remember that the measured expansion and predicted contraction are small, on the order of a few percent, and are within the errors of theory and experiment.

ORDERED HYDROGEN ADSORPTION STRUCTURE

With the adsorption of H, only slight changes were observed in the integral-order I - V curves, and the fractional-spot intensities were quite weak. This suggests that any reconstruction (i.e., lateral rearrangement of the metal atoms) is small and that the metal-metal interlayer distances do not change appreciably from the clean case. We therefore have concentrated on the location of the H atoms in our structural search. The Pd layers were not allowed to reconstruct, and Pd-Pd interlayer distances were varied near their values for the clean surface.

A model of the Pd(111) surface with an outline of the $(\sqrt{3} \times \sqrt{3})R30^\circ$ unit mesh is shown in Figs. 1 (top view) and 2 (side view). The three outermost layers of Pd atoms are labeled according to the "abc" stacking sequence of an fcc lattice. Six different types of high-

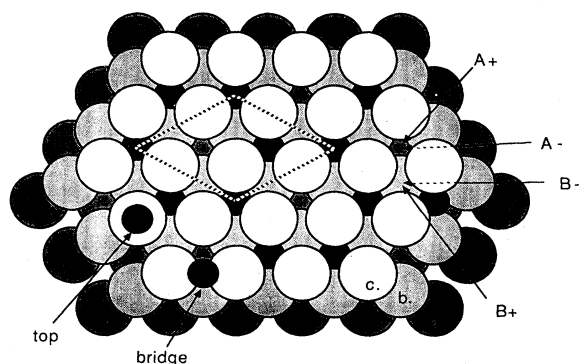


FIG. 1. Arrangement of the three outermost layers of Pd(111) in the fcc stacking arrangements, *abc*. The $(\sqrt{3} \times \sqrt{3})R30^\circ$ unit mesh is outlined. The various sites considered are shown, top, bridge, and threefold. The latter are designated $A+$, $A-$, $B+$, and $B-$, where the $+$ and $-$ symbols designate surface and subsurface (between first and second metal layers) sites and A and B designate above third- (a) and second- (b) layer metal atoms, respectively.

symmetry sites need to be considered. They are the top site, the bridge site, and four types of threefold symmetrical sites. The latter are classified as type A (above an a -type metal atom—a Pd atom in the third metal layer) or B (above a b -type metal atom—a Pd atom in the second

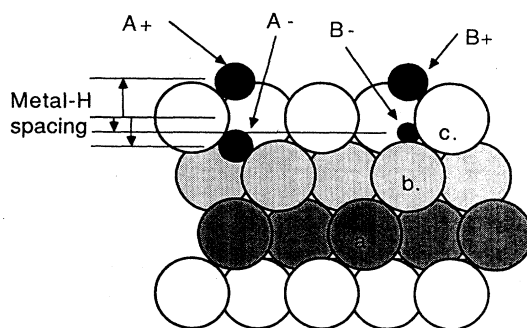


FIG. 2. As in Fig. 1, except side-on view. The figure is in the (011) plane and contains one of the sides of the $(\sqrt{3} \times \sqrt{3})R30^\circ$ unit mesh.

metal layer). For both A and B types there are two sites, namely above the surface (designated with $+$ and called surface site) and between the first two metal layers (designated with $-$ and called subsurface site). The $A+$, $A-$, $B+$, and $B-$ sites can also be referred to as the tetrahedral surface, octahedral subsurface, octahedral surface, and tetrahedral subsurface sites, respectively.

First we consider "single-site" geometries, i.e., those with all the H in the same site. Double occupancy in a molecular sense is excluded since the adsorption is dissociative. Thirteen possibilities are listed in Table I. There

TABLE I. Single-site $(\sqrt{3} \times \sqrt{3})R30^\circ$ structures considered. Information concerning interlayer spacings is reported in two rows, in units of Å. The first row lists the range of spacings tried in the format (start, stop, step interval). The second row lists the actual value at which the R factor is at a minimum. Metal-H spacings reported are the distance of the H atom above (+) or below (-) the plane of the first layer of Pd atoms. Metal-metal spacings are expansion (+) or contraction (-) relative to the bulk value.

Type	R factor	Metal-H spacing	Δd_{12}
$2A+$	0.228	0.5,1.5,0.5	0.025,0.075,0.025
		0.80	0.03
$2A-$	0.305	-1.62,-0.62,0.05	0.025,0.075,0.025
		-1.57	0.05
$2B+$	0.283	0.5,1.5,0.05	0.025,0.075,0.025
		0.90	0.03
$2B-$	0.264	-1.62,-0.62,0.05	0.025,0.075,0.025
		-1.02	0.03
$1A+$	0.224	0.5,1.5,0.05	none
		0.85	0.05
$1B+$	0.298	none	none
		0.80	0.05
$1A-$	0.297	-0.62,-1.62,0.05	none
		-0.82	0.05
$1B-$	0.252	-1.22,-1.02,0.1	0.0,0.075,0.025
		-1.12	0.05
2 top site	0.281	0.6,2.2,0.1	none
		1.40	0.05
2 bridge site	0.258	0.6,1.4,0.1	none
		1.00	0.05
2 bridge site	0.258	0.6,1.4,0.1	none
		1.40	0.05
2 bridge site	0.261	0.6,1.4,0.1	none
		1.40	0.05
2 bridge site	0.258	0.6,1.4,0.1	none
		1.00	0.05

is only one unique way of placing two H atoms in the $(\sqrt{3} \times \sqrt{3})R30^\circ$ unit mesh in top sites. This is also true for each of the four threefold sites, $A+$, $A-$, $B+$, and $B-$. For bridge sites, there are four inequivalent ways of filling the unit mesh with two H atoms. In addition to these nine possibilities the $A+$, $A-$, $B+$, and $B-$ sites are considered with only one H in the unit mesh ($\Theta = \frac{1}{3}$). (The sensitivity of LEED to H-H distances in these single-site geometries was assessed by computing the R factor between two sets of theoretical I - V curves. These curves were computed for identical local geometries, with the only difference being that one is at a coverage $\Theta = \frac{1}{3}$ and the other is at $\Theta = \frac{2}{3}$. For all four types of threefold sites discussed above, this R factor was less than 0.05. Although this demonstrates that LEED is less sensitive to H-H distances than Pd-H distances, it does permit disordered H to be handled in a manner discussed below.) Table I lists the geometry type, the best R factor, the distance of the H atom above (+) or below (-) the first Pd layer, and the distance Δd_{12} between the first and second metal layers relative to the standard bulk value of 2.246 Å. The distances, together with their beginning point, ending point and step size, are given in Å.

Occasional checks on Δd_{23} were made. In all cases this parameter remained at 0.00 Å, as in the clean structure. The distance Δd_{12} was varied more frequently but, in general, remained near the clean surface value. For these "single-site" structures, it is clear that the $A+$ site gives the best R factor. The distance of the H above the Pd metal layer (0.80 ± 0.10 Å) corresponds to a metal-H bond length of 1.78 ± 0.05 Å.

Since the EAM predicts simultaneous occupation of $A+$ and $A-$ sites, we also consider "two-site" ordered structures with one H in a subsurface site and one in a surface site. These structures have 50% subsurface occu-

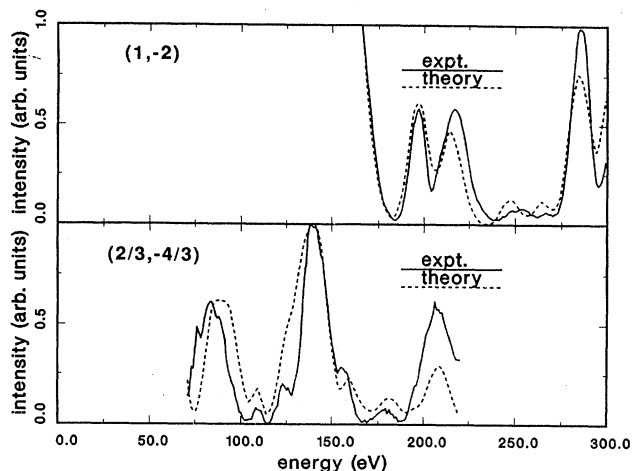


FIG. 3. Representative comparisons of theoretical and experimental I - V curves for the structure with the best overall R factor, $A+A-$ /same. One integral and one fractional beam are shown.

pation. For completeness, we also consider structures in which both H are in the same plane, but in different types of sites. The two-site ordered structures are listed in Table II. Note that there are two ways of populating the $A+A-$ combination: The two H atoms occupy surface and subsurface sites above either the same third-layer metal atom ($A+A-$ /same) or adjacent ones ($A+A-$ /other). An equivalent statement can be made for the $B+B-$ combination. Therefore, there are a total of eight of these "two-site" combinations to be considered.

Four of these combinations gave low R factors. They are $A+B+$ ($R=0.232$), $A+B-$ ($R=0.222$),

TABLE II. Two-site $(\sqrt{3} \times \sqrt{3})R30^\circ$ structures considered. Information concerning interlayer spacings is reported in two rows, in units of Å. The first row lists the range of spacings tried in the format (start, stop, step interval). The second row lists the actual value at which the R factor is at a minimum. Metal-H spacings reported are the distance of the H atom above (+) or below (-) the plane of the first layer of Pd atoms. Metal-metal spacings are expansion (+) or contraction (-) relative to the bulk value.

Type	R factor	Metal-H spacing (1)	Metal-H spacing (2)	Δd_{12}
$A+B+$	0.232	0.5,1.5,0.05	0.5,1.5,0.05	0.025,0.075,0.025
		0.85	0.85	0.03
$A-B-$	0.253	0.5,1.5,0.05	0.5,1.5,0.05	0.025,0.075,0.025
		0.85	0.85	0.03
$A+A-$ /same	0.221	0.6,1.0,0.05	-0.72,-1.52,0.05	none
		0.80	-1.22	0.05
$A+A-$ /other	0.237	0.6,1.0,0.05	-0.72,-1.52,0.05	none
		0.80	-1.17	0.05
$A+B-$	0.222	0.6,1.0,0.05	-0.72,-1.52,0.05	none
		0.80	-1.02	0.05
$B+A-$	0.283	0.6,1.0,0.05	-0.72,-1.52,0.05	none
		0.85	-0.72	0.05
$B+B-$ /same	0.272	0.6,1.0,0.05	-0.72,-1.52,0.05	none
		0.85	-1.12	0.05
$B+B-$ /other	0.271	0.6,1.0,0.05	-0.72,-1.52,0.05	none
		0.80	-1.12	0.05
$A+A-$ /mix ^a	0.222	0.5,1.5,0.5	-0.62,1.62,0.05	none
		0.80	-1.22	0.05

^aThe minimum of the R factor for the mixture (incoherent sum) of $A+$ and $A-$ occurs at 20% subsurface occupation (see Fig. 4).

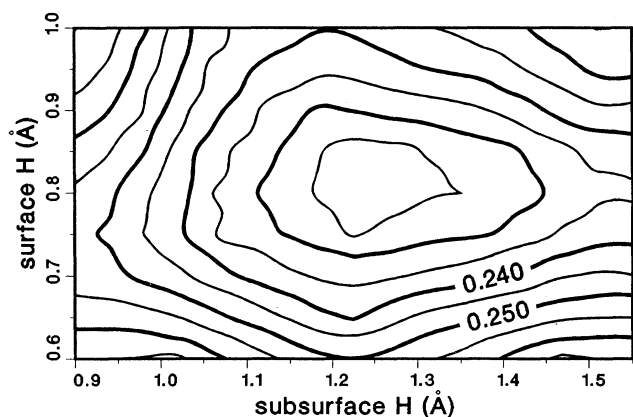


FIG. 4. Contour plot of R factor for $A + A -$ /same structure (see text) with variation of surface and subsurface H-to-Pd layer spacings. The spacings are defined as the distance between the plane of the first layer of palladium atoms and either the surface or the subsurface hydrogen.

$A + A -$ /same ($R=0.221$), and $A + A -$ /other ($R=0.237$). The $A + B -$ combination gives a reasonable bond length from the surface and subsurface hydrogens to the first-layer Pd atoms. However, the bond length from the subsurface H to the Pd atom directly below it is unphysically short (1.27 Å). This would place the H closer to the Pd atom than even the muffin-tin radius (1.38 Å). In addition, when the R factors for the integral and fractional beams are minimized separately, different solutions are obtained. These considerations indicate a spuriously low R factor, and we therefore exclude this geometry from further consideration.

Calculated $I-V$ spectra for the $A + A -$ /same structure, which produced the lowest overall R factors in this work, are compared to experiment in Fig. 3. One fractional- and one integral-order beam are shown. They were chosen to be displayed in the figure because they represent for this structure agreement between theory and experiment that is typical, i.e., neither the best nor the worst. The sensitivity of the overall R factor of this structure to surface and subsurface H vertical positions is exhibited in the contour plot of Fig. 4. Note that the R factor is more sensitive to the surface H position, but variations in either show a clear minimum.

We note that the two structures $A + A -$ /same and $A + A -$ /other have similar R factors. More importantly, the R -factor minimizations yield essentially identical local geometries (the location of the H atoms with respect to the Pd atoms). In fact, the only difference in the structures is in the location of the H atoms relative to each other; as discussed parenthetically above, it is difficult to resolve such details of the structure by LEED.

DISORDERED HYDROGEN ADSORPTION STRUCTURE

The EAM predicts^{5,6} that substantial vertical disorder exists at 82 K, despite near-perfect lateral order. That is, hydrogen may occupy $A +$ and $A -$ sites on a random basis, while still maintaining the $(\sqrt{3} \times \sqrt{3})R 30^\circ$ lateral

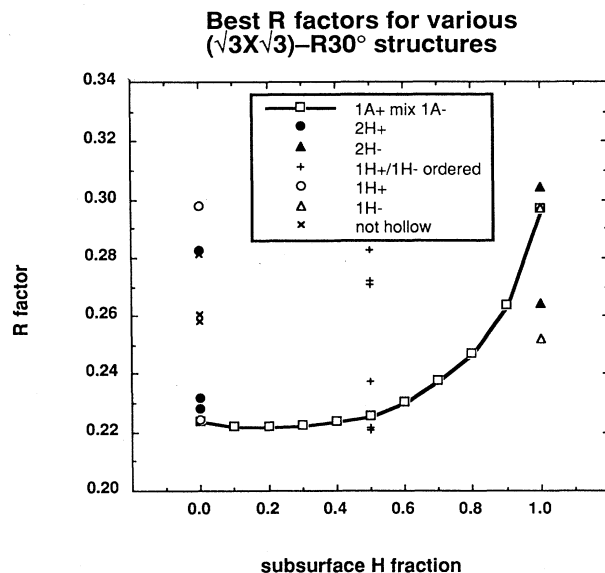


FIG. 5. R factors for the various $(\sqrt{3} \times \sqrt{3})R 30^\circ$ hydrogen structures vs subsurface occupation. The solid line is obtained by summing different percentages of $I-V$ curves from $A +$ (surface) and $A -$ (subsurface) 1H structures. The 21 individual points are listed in Tables I and II.

periodicity. The ordered structures discussed previously can account for subsurface occupations of 0%, 50%, and 100%, but other proportions cannot be handled in the $(\sqrt{3} \times \sqrt{3})R 30^\circ$ cell. The similarity of theoretical $I-V$ curves for $\Theta = \frac{1}{3}$ and $\Theta = \frac{2}{3}$ single-site geometries in the previous section suggests the possibility of mimicking vertical disorder by incoherently summing the theoretical $I-V$ curves for a surface (e.g., $1A +$) and a subsurface (e.g., $1A -$) geometry. The incoherent sum may be performed at any subsurface occupation. To assess the validity of this approach, the incoherent sum at 50% $1A +$ and 50% $1A -$ was compared to the ordered $A + A -$ structure by computing the R factor between the two sets of theoretical $I-V$ spectra. This R factor was found to be small (< 0.1), giving us confidence to go ahead and compare the incoherent-mixture calculations to experiment. The solid line in Fig. 5 shows the R factor comparing the incoherent sum with experiment as a function of subsurface occupation (the percentage of $1A -$ in the mixture). For pure $1A +$, there is 0% subsurface occupation, and the R factor and resulting geometry are as given in Table II. As the subsurface component is introduced, the R factor decreases slightly, reaching a minimum at approximately 20% subsurface occupation. For each percentage of subsurface H the R factor plotted in Fig. 5 represents an optimized geometry. The R factor increases slightly as 50% subsurface occupation is reached, and then increases rapidly beyond 60%, reaching its highest value at the large R factor found for the simple $A -$ structure. Even though the pure- $A -$ structure gave a poor R factor, more than 50% of the H can nevertheless be in this site and still yield a good R factor, provided that the remainder is in the $A +$ site. Note that the best R factors for two ordered structures at 50% subsurface occu-

pation, $A + A -$ /same and $A + A -$ /other, bracket the R factor at 50% on the solid line of Fig. 5. This not only supports the validity of the interpolation, but also provides a measure of its error which suggests that subsurface occupations anywhere from 0% to 60% are consistent with our LEED analysis.

DISCUSSION

Table III lists the H-metal distance for the five best structures determined in the present work together with determinations from previous work on other metal surfaces. In the previous work, the H was determined to be in threefold hollow sites in the cases of hexagonal substrates, and pseudothreefold hollow sites for the (110) surfaces (two bond lengths are listed in the case when the H sits off center over the threefold site). The Ru(0001) work was for (1×1) and disordered structures, over a range of coverages, giving rise to a range of bond lengths. The first entry in the table is for the best structure of the "single-site" types listed in Table I, namely $A +$. The next four entries are discussed below.

As can be seen from Table III, the bond length and geometry for H in the $A +$ site are consistent with the prior determinations on other surfaces using various techniques. Of the surface sites, this is the most favored by the EAM calculations. One other site, the $A -$, was predicted to be marginally lower in energy, but relatively poor R factors were achieved for geometries with only the $A -$ site occupied. To understand this apparent disagreement, we need to consider another prediction of the EAM consistent with ESD measurements: the presence of substantial vertical disorder. The EAM predicts that the $A +$ and $A -$ sites are nearly degenerate in energy and that the barrier between them is small. As a consequence, 33% of the H is in surface sites at 75 K, while the remainder is in the subsurface octahedral ($A -$) sites.

The site degeneracy and vertical disorder predicted by

the EAM was strong motivation for us to consider the two-site structures listed in Table II. Three of these have sufficiently low R factors to deserve consideration along with the single-site geometry, $2A +$, and are therefore listed in Table III. All three have one hydrogen in the $A +$ site. Two have the second hydrogen in the $A -$ subsurface site, either directly below the surface hydrogen (same) or in the adjacent site (other). The fifth possible structure listed in Table III represents a mixture of $A +$ and $A -$ sites. The lowest R -factor was found at approximately 20%, but mixtures between 0 and 60% gave adequately low R factors with only slight changes in the adsorption geometry.

For all five of the possibilities listed in Table III for the present work the geometry of the surface H relative to its three nearest-neighbor Pd atoms is essentially the same. That is the $\text{Pd}_1\text{-H}$ length is between 1.78 and 1.80 Å corresponding to a distance between the surface H and the first palladium plane of 0.80 to 0.85 Å. This agrees very well with previous structures determined by other authors for various surfaces as listed in Table III.

For those candidate structures with subsurface hydrogen, it is always found between 1.17 and 1.22 Å below the first Pd plane, corresponding to a $\text{Pd}_1\text{-H}$ length between 1.97 and 2.00 Å and a $\text{Pd}_2\text{-H}$ length between 1.96 and 1.92 Å. This is close to the Pd-H distance in the bulk α (solid solution) phase 1.95 Å and in the β (hydride) phase 2.01 Å.

Figure 5 shows the R factors for the structures listed in Table I and II. It is clear that many of the structures can be eliminated by their large disagreement with experiment. However, the ideal situation, the elimination of all but one geometry, clearly has not been achieved. From the point of view of the EAM results, it is important to note that structures with considerable vertical disorder, as approximated here, agree with the present LEED experiment. Our present findings are consistent with the EAM prediction of substantial subsurface H in the $A -$ site and partial occupation of the surface $A +$ site at a total coverage of $\Theta = \frac{2}{3}$.

TABLE III. Metal—Hydrogen bond lengths. Bond length from surface (+) and subsurface (−) hydrogen to palladium atoms in the first-, Pd_1 , and second-, Pd_2 , layer metal atoms. References for the previous determinations are listed in square brackets.

Surface	Unit mesh	$\text{Pd}_1\text{-H}+$	$\text{Pd}_{1,2}\text{-H}$	Notes
Pd(111)	$(\sqrt{3} \times \sqrt{3})\text{-1H,2H}$	1.78 Å		$A +$, best single site
		1.80		$A + B +$
		1.78	2.00, 1.92	$A + A -$ /same
		1.78	1.97, 1.96	$A + A -$ /other
		1.78	2.00, 1.92	$A +$ and $A -$ mixture
Pt(111)	(1×1)	1.76		EELS [13]
		1.9		He scattering [16]
Ru(0001)	$0.2 < \Theta < 1.0$	1.78-1.91		VLEED [17]
Ni(111)	$(2 \times 2)\text{-2H}$	1.84		LEED [14]
		1.65		transmission channeling [18]
Pd(100)	$c(2 \times 2)$	2.00		transmission channeling [19]
Pd(100)	(1×1)	1.97		transmission channeling [19]
Rh(110)	$(1 \times 1)\text{-2H}$	1.84		LEED [23]
Pd(110)	$(2 \times 1)\text{-2H}$	1.99, 2.11		LEED [24]
Ni(110)	$(2 \times 1)\text{-2H}$	1.72		LEED [25]

CONCLUSION

LEED I - V curves have been obtained for the Pd(111)- $(\sqrt{3}\times\sqrt{3})R30^\circ$ -2H structure at 82 ± 1 K at normal incidence. The best agreement with calculated spectra occurs with all H in the threefold hollow surface sites above third-layer metal atoms ($A+$ sites) or in mixtures containing H in this site and in the $A-$ subsurface sites (octahedral sites between the first and second metal layers). These sites are also favored by the embedded-atom-method calculations of Daw and Foiles.⁵

Occupation of other sites, such as bridge, top, subsurface tetrahedral ($B-$ sites), and threefold hollow surface sites above second-layer metal atoms ($B+$ sites), is ruled out, in agreement with the EAM. For all structures with good R factors, the H in $A+$ sites is a vertical distance of 0.80 to 0.85 Å above the topmost Pd layer, corresponding to a metal—H bond length of 1.78 to 1.80 Å. (Vertical distances are determined within ± 0.10 Å corresponding to metal—H distances within ± 0.05 Å.) Among these, the best agreement was obtained with the two-site $A+A-$ ordered structure. The metal—H bond lengths for the subsurface hydrogen are 2.00 Å from the first-layer Pd atoms and 1.92 Å from the second-layer Pd atoms. The subsurface hydrogen is a vertical distance of 1.22 Å below the top Pd layer. This may be compared with the ideal octahedral site, which is the site occupied in the bulk hydride, at 1.12 Å below the top Pd layer if the Pd—Pd interlayer spacing takes on the bulk value of 2.25 Å (1.15 Å for Pd planes separated by the slightly expanded value of 2.3 Å as determined by the present work). At low coverage, the EAM gives this distance to

be 0.7 Å; with higher coverage, the H atom moves to the geometrical center of the octahedral site.

The EAM predicts good lateral periodicity, but substantial vertical disorder: 67% subsurface and 33% surface occupation at 74 K, i.e., near our experimental temperature of 82 K. We made use of the relatively small contribution of hydrogen-hydrogen multiple scattering to model vertical disorder in the LEED calculations. Our results are consistent with a subsurface occupation in the range 0–60%, and are generally less specific in terms of percentage of surface and subsurface occupation than the ESD measurements of Kubiak and Stulen which confirmed the presence of substantial subsurface occupation and vertical disorder.⁴ Cooling the sample to approximately 20 K should aid in the determination of the H geometry by freezing out the vertical disorder in the Pd(111)- $(\sqrt{3}\times\sqrt{3})R30^\circ$ -2H structure, and may permit determining the structure for the simpler, and somewhat less stable, Pd(111)- $(\sqrt{3}\times\sqrt{3})R30^\circ$ -1H structure.

ACKNOWLEDGMENTS

The authors thank R. H. Stulen, M. S. Daw, S. M. Foiles, L. D. Roelofs, and H. Ohtani for very helpful discussion and B. V. Hess for developing the hardware and software for video data collection and for technical assistance with the vacuum system. This work was supported by the U.S. Department of Energy under Contract No. DE-AC04-76DP00789 and by the Director, Office of Energy Research, Office of Basic Energy Sciences, Materials Sciences Division of the U.S. Department of Energy under Contract No. DE-AC03-76SF00098.

*Present address: Lawrence Livermore National Laboratory, Livermore, CA 94550.

¹J. W. Davenport and P. J. Estrup, in *The Chemical Physics of Solid Surfaces and Heterogeneous Catalysis*, edited by D. A. King and D. P. Woodruff (Elsevier, Amsterdam, 1989), Vol. 3A.

²K. Christmann, *Surf. Sci. Rep.* **9**, 1 (1988).

³W. Eberhardt, F. Greuter, and E. W. Plummer, *Phys. Rev. Lett.* **46**, 1085 (1981); W. Eberhardt, S. G. Louie, and E. W. Plummer, *Phys. Rev. B* **28**, 465 (1983).

⁴G. D. Kubiak and R. H. Stulen, *J. Vac. Sci. Technol. A* **4**, 1427 (1986).

⁵M. S. Daw and S. M. Foiles, *Phys. Rev. B* **35**, 2128 (1987).

⁶M. S. Daw and M. I. Baskes, *Phys. Rev. Lett.* **50**, 1285 (1983); *Phys. Rev. B* **29**, 6443 (1984).

⁷T. E. Felter, S. M. Foiles, M. S. Daw, and R. H. Stulen, *Surf. Sci. Lett.* **171**, L379 (1986).

⁸W. Ho, N. J. DiNardo, and E. W. Plummer, *J. Vac. Sci. Technol.* **17**, 134 (1980).

⁹H. Conrad, R. Scala, W. Stenzel, and R. Unwin, *J. Chem. Phys.* **81**, 6371 (1984).

¹⁰M. A. Barteau, J. Q. Broughton, and D. Menzel, *Surf. Sci.* **133**, 443 (1983).

¹¹C. M. Mate, B. E. Bent, and G. A. Somorjai, in *Hydrogen Effects in Catalysis*, edited by Z. Paál and G. Menon (Dekker,

New York, 1988), Chap. II, p. 65; C. M. Mate and G. A. Somorjai, *Phys. Rev. B* **34**, 7417 (1986).

¹²H. Conrad, M. E. Kordes, R. Scala, and W. Stenzel, *J. Electron Spectrosc. Relat. Phenom.* **38**, 289 (1986).

¹³A. M. Baro, H. Ibach, and H. D. Bruchman, *Surf. Sci.* **88**, 384 (1979).

¹⁴K. Christmann, R. J. Behm, G. Ertl, M. A. Van Hove, and W. H. Weinberg, *J. Chem. Phys.* **70**, 4168 (1979).

¹⁵M. J. Puska, R. M. Nieminen, M. Manninen, B. Chakraborty, S. Holloway, and J. K. Nørskov, *Phys. Rev. Lett.* **51**, 1081 (1983).

¹⁶I. P. Batra, J. A. Barker, and D. J. Auerbach, *J. Vac. Sci. Technol. A* **2**, 943 (1984); analyzed data from J. Lee, Ph.D. thesis, University of Chicago 1981; J. Lee, J. P. Cowin, and L. Wharton, *Surf. Sci.* **130**, 1 (1983).

¹⁷M. Lindroos, H. Pfnür, and D. Menzel, *Surf. Sci.* **192**, 421 (1987).

¹⁸K. Mortensen, F. Besenbacher, I. Stensgaard, and W. R. Wampler, *Surf. Sci.* **205**, 433 (1988).

¹⁹F. Besenbacher, I. Stensgaard, and K. Mortensen, *Surf. Sci.* **191**, 288 (1987).

²⁰K. H. Ernst and K. Christmann, *Verh. Dtsch. Phys. Ges.* **2**, 0 (1987); (unpublished).

²¹M. A. Passler, B. W. Lee, and A. Ignatiev, *Surf. Sci.* **150**, 263 (1985).

- ²²W. Moritz, R. Imbihl, R. J. Behm, G. Ertl, and T. Matsushima, *J. Chem. Phys.* **83**, 1959 (1985).
- ²³W. Oed, W. Puchta, N. Bickel, K. Heinz, W. Nichtl, and K. Mueller, *J. Phys. C* **21**, 237 (1988).
- ²⁴M. Skottke, R. J. Behm, G. Ertl, V. Penka, and W. Moritz, *J. Chem. Phys.* **87**, 6191 (1987).
- ²⁵W. Reimer, V. Penka, M. Skottke, R. J. Behm, G. Ertl, and W. Moritz, *Surf. Sci.* **186**, 45 (1987).
- ²⁶T. E. Felter, R. H. Stulen, M. L. Koszykowski, G. E. Gdowski, and B. Garrett, *J. Vac. Sci. Technol. A* **7**, 104 (1989).
- ²⁷M. A. Van Hove, W. H. Weinberg, and C.-M. Chan, *Low-Energy Electron Diffraction Experiment, Theory and Surface Structure* (Springer-Verlag, Berlin, 1986).
- ²⁸M. A. Van Hove and S. Y. Tong, *Surface Crystallography by LEED* (Springer, New York, 1979).
- ²⁹H. Ohtani, M. A. Hove, and G. A. Somorjai, *Surf. Sci.* **187**, 372 (1987).
- ³⁰W. Moritz (private communication).
- ³¹Reference 28, p. 237.
- ³²Properties of palladium hydride can be found in J. D. Fast, *Gases in Metals* (Macmillan, New York, 1976), pp. 39–42. F. A. Lewis, *The Palladium-Hydrogen System* (Academic, New York, 1967); E. Wicke, H. Brodowsky, and H. Züchner, in *Hydrogen in Metals II*, edited by G. Alefeld and J. Vökl (Springer, New York, 1978), p. 73.
- ³³G. E. Gdowski, T. E. Felter, and R. H. Stulen, *Surf. Sci. Lett.* **181**, L147 (1987).